CFD Letters 15, Issue 11 (2023) 181-200

SEMARAK ILMU PUBLISHING

CFD Letters

Journal homepage:
https://semarakilmu.com.my/journals/index.php/CFD_Letters/index
ISSN: 2180-1363

Numerical Investigation and Comparison Between Internal and External Liquid Biofuel Pre-Evaporation in Micro Gas Turbine Chamber

Mohammed R. Abdulwahab[1,2], Khaled A. Al-attab[2,*] Mohamad Yusof Idroas[2]

[1] Department of Power Mechanical Engineering, Technical College of Mosul, Northern Technical University, Mosul, Iraq
[2] School of Mechanical Engineering, Engineering, Engineering campus, Universiti Sains Malaysia,14300 Nebong Tebal, Penang, Malaysia

ARTICLE INFO

Article history:
Received 16 May 2023
Received in revised form 21 June 2023
Accepted 19 July 2023
Available online 1 November 2023

Keywords:
Liquid Biofuels; CFD; Micro Gas Turbine; Combustion

ABSTRACT

Due to the current global crises related to fossil fuels (prices up and sources shortage) and in order to diminish the remnants and the negative effects of harmful gas emission (CO and NOx), the fielded researchers and academics try to find alternative source of fossil fuel. Bio fuels consider one of promised source of clean energy. Palm vegetable oil widely separated in Malaysia which considered one of dominant production of this oil globally. Atomization and evaporation radically represent a challenge when using liquid fuel especially fuels with high viscosity and density which is not easy to atomize and evaporate without pre-heating or blende it. A numerical investigation has been proposed to do comparison between two different external evaporative chamber and internal evaporation without using conventional liquid fuel evaporation methods. Findings revealed that both configurations have a good performance in term of emission concentrations and turbine inlet temperature (TIT) which was about 899 C with chamber using internal recycle tube evaporation with CO emission about 183 ppm with outer pre-evaporation chamber. Chamber with internal evaporation was chosen due to technical and fabrication reasons. Besides that, a six different inlet and exhaust ducting ports tested with the chosen chamber with internal recycle tube evaporation chamber, all configurations revealed a non-symmetrical flame flow near chamber exhaust which is not desirable as it will cause turbine unstable operation. The configuration with square duct exhaust was suitable with stable and symmetric flame flow field and slight small CO emission about 312 ppm.

1. Introduction

More than 80% of the world's energy requirements are currently met by the consumption of fossil fuels. This Allowed rapid industrial development towards full automation, but the other aspects of contemporary human existence became highly dependent on fossil fuel consumption. Coal, natural gas, and oil are the three primary fossil fuels used in Malaysia to generate electricity. As the depletion of fossil fuels is inevitable, the rapid increase in energy demand raises serious concerns about alternative fuels. Moreover, the combustion of fossil fuels is the leading cause of the increase in net greenhouse gas emissions [1]. Global warming and other environmental issues have intensified due

* *Corresponding author.*
E-mail address: khaledalattab@yahoo.com (Khaled A. Al-attab)

https://doi.org/10.37934/cfdl.15.11.181200

to the increase in greenhouse gas emissions from the combustion of fossil fuels. Thus, the use of alternative fuels instead of conventional fuels and the implementation of efficient combustion technologies became a necessity [2-4].

Biomass renewable fuel resources have recently been proposed as an alternative to fossil fuels for mitigating global warming due to the fact that they have no effect on greenhouse gas emissions. Malaysia has a wealth of biomass resources, such as waste from the oil palm industry, that can be used to generate electricity for industrial production [5]. In addition, extensive research has been conducted on biogas derived from wastewater effluent, municipal solid wastes (MSW), animal waste, and agricultural residues for combined heat and power (CHP) applications [6-10]. However, liquid biofuels are crucial because they can effectively replace petroleum products in the transportation, aviation, and power generation industries. Before they can be implemented in the aviation sector, renewable liquid biofuels must be thoroughly studied and characterized. Butyl nonanoate biofuel was investigated experimentally and compared to hydrogenated renewable jet (HRJ) fuel and JP-8 fuel. The phase doppler particle technique was used to investigate the properties of fuel atomization. Butyl nonanoate produced lower CO emissions than JP-8, in contrast to HRJ biofuel, which produced higher CO emissions than JP-8 [11].

Empty fruit bunch (EFB), palm mesocarp fibre (PMF), and palm kernel shell (PKS) from a palm oil mill facility should be investigated as a possible raw material for co-firing with coal. Co-firing is a low-cost, low-risk method for utilizing biomass in the generation of electricity. A comparative analysis of the existing co-firing biomass processes around the globe in order to investigate the feasibility of using palm oil wastes with coal was conduct. To accomplish successful co-firing of biomass and coal, it is necessary to understand the characteristics of the feedstock before implementing various pre-treatment strategies. Co-firing palm oil waste with coal is recommended in Malaysia because palm oil residues can reduce greenhouse gases, NOX, and SOX. Cofiring palm oil wastes in existing coal-fired power plants is one of the feasible ways to be implemented, as it serves to reduce the excessive consumption of fossil fuels. Malaysia appears to be on the correct track to maximize the use of palm oil wastes in either a standalone biomass power plant or a co-firing power plant, according to the findings. The enhanced utilization will further mitigate the negative impact of the untreated palm oil mill residues' greenhouse gas emissions [12].

Similar results were observed when jet-A1 was blended with biofuels, with a decrease in CO emissions and a minor increase in NOx emissions [13,14]. Medium or Intensive low oxygen dilution (MILD) is yet another technology being studied to improve the combustion of liquid biofuels. An experimental investigation investigated the combustion of pre-vaporized liquid fuels in a reverse-flow MILD combustor under high pressures. Results revealed that the stability of combustion is dependent predominantly on fuel type, with n-heptane being the most unstable fuel due to its fast ignition under different high-pressure conditions [15]. Another combustion technology getting more attention recently is the flameless combustion, which can be achieved through intensive internal heat recirculation or the implementation of highly preheated air supply. Experimental and numerical analysis of combustor with double stage combustor investigated flameless combustion with liquid fuels, with variable inputs of thermal heat in the range of 20-60 kW, and with heat intensity release of 5–15 MW/m3. Using computational fluid dynamics (CFD), another study simulated the combustion and emission characteristics of kerosene, diesel, and petrol. The flow analysis reveals that limiting the diameter of the exit port of the primary chamber can increase the recirculation rate of combustion products, which contributed to the attainment of flameless combustion mode [16].

Swirl flow was also proposed to improve heat circulation, enabling flameless combustion with heat release intensities between 5.4 and 21 MW/m3 to be achieved with kerosene fuel. Increases in chamber radius, recirculation of combustion products, and fuel residence time were shown to improve flameless combustion by CFD analysis [17]. The Stirling engine was developed to assess the viability of recovering residual heat from biomass to generate energy. In order to design an initial computational model of Stirling engine for low-temperature heat waste recovery, a Computational Fluid Dynamics (CFD) simulation test was conducted. The CFD model was validated against the experimental model and reveals an average deviation of 6.11 percent. This result demonstrates that the computational model can be used to evaluate the performance of Stirling engines as biomass-based industrial furnaces' waste heat recovery systems for low-grade temperature heat sources [18]. A substantial amount of research on liquid biofuels is devoted to gas turbine technology, which stands to gain the most from these fuels. The combustion characteristics of Palm methyl ester (PME) as a replacement fuel for gas turbines were investigated experimentally with preheated air at 673 K. The results indicated that the combustion characteristics of PME are comparable to those of diesel fuel, whereas NOx emissions were lower when PME was used in place of diesel fuel in gas turbines [19]. Another experimental study on gas turbine fuels compared two liquid fuels: biodiesel and a mélange of biodiesel and bio-oil derived from pyrolysis. These two fuels were measured against paraffin as the standard. In terms of combustion stability, the saturated blend appears to be a viable option for gas turbine power generation [20]. Similarly, blends of kerosene and bio-oil derived from waste tire pyrolysis (up to 50 percent) achieved sustained turbine operation, albeit with increased CO and NOx emissions [21].

For micro gas turbine (MGT) applications on a smaller scale, combustion analysis of a highly oxygenated and economically viable viscous fuel, such as glyceollin, was performed. The results revealed that this fuel provided environmental benefits in the form of reduced NOx emissions and particulate matter concentration [22]. Utilizing well-established turbocharger technology for the development of small-scale MGT is a promising option for reducing the price of MGT. However, a small combustion chamber must be created because turbochargers lack one. Using CFD simulation, the combustion chamber for a turbocharger-based two-stage MGT was designed. Using species transport and non-premixed combustion models, different chamber and flame tube geometries were investigated in order to determine the optimal chamber design [23]. Fuel spray patterns and atomization quality with different injector diameters and fuel flow rates were investigated experimentally to determine their effect on combustion quality [24].

The extension of the flame tube with a portion for fuel pre-evaporation resulted in low CO emissions of 99 ppm and NOx emissions of 13 ppm at turbine inlet temperature (TIT) of 1329 K when using diesel fuel [24]. Another simulation [25] investigated the MGT life cycle analysis, greenhouse effect, and combustion characteristics of natural gas compounds containing ammonia and methanol. Liquid biofuel combustion requires a specific fuel discharge characteristic. For reciprocating internal combustion engines, the ignition delay caused by the use of fuels with a higher viscosity, such as biodiesel versus fossil diesel, is a significant issue [26]. Due to the essentially different nature of combustion in gas turbines, which utilizes steady-state combustion rather than intermittent combustion, this concern is irrelevant. Despite this, poor fuel atomization and evaporation when using viscous liquid biofuels remains a significant issue, as fuels with poor evaporation require a significant extension of the flame, necessitating modifications to the geometry of the MGT combustion chamber.

In order to utilize low-grade liquid biofuels in MGT, it is essential to investigate the fuel evaporation mechanism and how to improve it. An investigation was conducted into a droplet evaporation model of biodiesel fuels based on continuous mixture theory. The model was compared to experiments with solitary suspended droplets and was found to be within 3% of the measurements [27]. Using a constant volume vessel with a single-hole nozzle, the evaporation spray and combustion characteristics of a broad range of ethanol–gasoline mixtures (E0-E100) were studied. The results indicated that the evaporation rate of ethanol was greater than that of petrol; therefore, when blending two fuels with differing boiling points, distinct stratified vapor layers are formed [28].

The viscosity of vegetable oil is approximately one order of magnitude greater than that of diesel (3.6 mm2/s), whereas the viscosity of biodiesel is only marginally greater than diesel (5.9 mm^2/s) [29]. Utilizing fuel pre-heaters to reduce the viscosity of biofuels is one of the earliest techniques in use. However, external fuel preheat methods can result in fuel fouling and blockage due to fuel coking and pyrolysis on the heated surfaces, in addition to the formation of gas pockets within the fuel lines, which can cause pressure fluctuations [29]. Using diesel as the standard fuel, the MGT performance was compared to externally pre-heated biodiesel and vegetable oil using electrical heaters [30]. A method of diesel evaporation without injectors for atomization was evaluated. The thermal power of superheated steam from a steam injector is used to evaporate liquid diesel from a container at the bottom of a burner that is appropriate for high viscosity fuels [30]. However, this was tested with an atmospheric burner, and its stability in gas turbine applications is debatable. Using Mie-scattering and laser-induced exciplex fluorescence (LIEF) optical techniques, the changes of spray patterns and vaporization behaviour for flash-boiling multi-hole injector spray over a broad spectrum of superheated conditions were studied. The vaporization of n-hexane was evaluated using the LIEF optical technique, which provided the relative amount of vapor throughout the spray transformation procedure. The correlations between aerosol structural change and extent of vaporization with increasing superheated degree provided excellent insight into the mechanisms responsible for the observed behaviours under conditions of flash boiling [31].

Using vibration analysis [32] and combustion acoustic analysis [33] to examine the effect of inadequate atomization of biofuels on the stability of combustion was also investigated. Experimentally, the dielectric-barrier-discharge (DBD) plasma actuator's capability for air flow-based controlling in micro combustors with haze generator was evaluated. Continuously generated plasma has a maximal temperature of 90 C and has a minimal effect on the characteristics of the flow, according to the results [34]. Using CFD modelling, neon-oxygen was investigated for the stabilization of hydrogen ignition under standard ambient ingestion conditions. Results indicated that the mean initial hydrogen temperature in neon-oxygen atmospheres was lower than in oxygen-argon environments [35].

Before testing the geometry experimentally, CFD modelling has demonstrated to be a valuable tool for optimizing turbine geometry and flow characteristics to increase the power coefficient of the turbine [36]. Using the Lagrangian particle tracking (LPT) method, the external and internal vaporization of single flash-boiling droplets were studied computationally. Numerous internal vaporization models included sub-models for calculating bubble number density with bubble growth rate and droplet rupture criterion. For the external vaporization model, heat transfer from droplet interior to droplet surface and from ambient gas to droplet surface were considered. It has been discovered that the nuclei of vapor droplets are a crucial factor in the transition from a metastable to a stable liquid phase [37].

Isopropanol-butanol-ethanol (IBE) was blended with diesel in varying proportions, then tested using the Mie-scattering method in a constant volume chamber. After combining IBE with diesel, spray evaporation characteristics vastly improve, according to experimental findings. Moreover, the ambient temperature had a significant effect on the spray evaporation of both pure diesel and IBE/diesel blends, with an increase in temperature resulting in smaller spray streams [38]. To enhance the pre-evaporation of liquid spray in confined spaces, electrostatic fields to control the location of electrically charged droplets of fuel have been studied [39]. Pre-evaporation pulse combustion using a porous medium burner is an additional method for enhancing liquid biofuel utilization. It was discovered that the minimum preheating temperature for complete evaporation and sustained combustion is approximately 1023 K, whereas the maximum flame temperature reached is approximately 1300 K [40].

The widespread use of compression ignition engines for heavy-duty applications is due to their superior fuel efficiency. However, this form of engine contributes to the production of NOx and soot emissions, which result in harmful environmental pollution to human health. The RCCI engine concept is still in its infancy, and numerous studies on the control of combustion and emission release are required. In addition, the operational range of RCCI engines is limited by their heat release rate (HRR) and peak pressure release rate (PPRR), as well as their poor combustion efficiency, which leads to high HC and CO emissions. The effect of single injection strategy on performance, combustion characteristics, and emissions was investigated. Converge V2.4, a 3D computational fluid dynamics (CFD) program, was used to conduct the study, which was based on the parameters of a single-cylinder, direct-injection Yanmar TF90 diesel engine. The results indicate that operating the engine at a lower engine speed is more conducive to diesel-ethanol combustion, which results in superior engine performance. This is because, at high engine speeds, the oxygen content in the cylinder is insufficient for complete combustion, leading to an increase in emissions [41].

EGR and multiple combustion phases were implemented to reduce NOx formation during combustion. The effect of attenuated preheated oxidizer variables on NOx emissions from methane combustion was investigated numerically. A Computational Fluid Dynamics (CFD) analysis was used to determine the effect of preheating fuel and air on combustion efficiency when an asymmetric vortex flameless burner is applied to various supply tangential air locations with varying oxygen concentrations. Utilized design parameters include attenuated N2 and CO2, oxygen concentrations of 10%, 7%, and 5%, and air temperatures of 300 K, 500 K, 700 K, and 900 K, respectively. The impact of air preheating on NOx emissions is greater than that of fuel preheating. The results of the analysis indicate that tangential air intake has a significant effect on combustion temperature and NOx emission [42].

Poor atomization of the viscous liquid fuel was a principal issue studied by researchers which is conversely affect the combustion quality, stability and hot gas emission. There are a lot of findings about this problem solutions like fuel pre-heating and mix with diesel and biodiesel. However, there is lack of studies on the internal pre-evaporation chambers associated with MGT for the direct utilization of low-grade liquid biofuels without the need for fuel pre-heating. This study investigates and compares novel designs of internal and external pre-evaporation chamber designs. Wide range of geometries and operation variables were optimized using CFD simulation. The new chamber design enables the direct use of low-grade liquid biofuels without any requirement for fuel pre-heat or blend with diesel.

This study aims at achieving two main objectives:

i. First, is to compare the external and internal pre-evaporation methods to optimize the evaporation of low-grade liquid biofuels in MGT combustion chamber.
ii. Second, is to optimize the inlet and outlet geometries of the combustion chamber using CFD simulation.

2. Methodology

Two chambers with different fuel evaporation configuration was tested, external revolve evaporation by connect the main combustion chamber with outer pre-evaporation chamber which was published previously [43] and internal evaporation inside combustion chamber itself which is consist of 3 annular cylinders from outside to inside respectively(air jacket, flame tube and recycle tube), recycle tube gas which is inside flame tube used to recirculate hot combustion gases through holes at recycle tube upper side. The optimum chamber case selected from first stage was examined with different air inlet and gas outlet ducting geometries. SOLD-WORKS software used to design chambers which then numerically analysed using ANSYS-Fluent software by set Species transport model and Discrete Phase Model (DPM). As for the fuel source material, palm oil is produced in abundance in Malaysia with high waste potential that can cause environmental concerns.

2.1 Fuel

Oil palm biomass, which is one of the most abundant lignocellulosic biomass in Malaysia, represents an alternative energy resource that can be exploited to reduce the dependency on fossil fuel whilst fulfilling the increasing energy demand [44].The palm oil industry is currently one of the major contributors to the Malaysian economy, which generates more than 311 million tons of lignocellulosic biomass wastes annually from palm oil plantation and milling activities [45]. Thermal properties of fuel which have been used to perform chamber simulation are listed in Table 1.

Table 1
Thermal properties of oil palm fuel at 30 °C [46]

Properties	Value
Density (kg/m^3)	885
Specific heat(J/Kg.°C)	1875
Viscosity (Pa.s)	57.85
Vaporization temperature (°C)	450
Boiling Point (°C)	510

The full molar fraction for the exhaust recycled gas was then calculated in Eq. (1) [43].

$$\frac{83}{12}C + \frac{11.43}{1}H + \frac{3}{16}O + \frac{2.47}{14}N + 25.62(O_2 + 3.76N_2) \rightarrow 5.69CO_2 + 1.23CO + 5.71H_2O + 16.55O_2 + 96.67N_2 \quad (1)$$

2.2 Chamber Geometry Parameters and Characterization

The first objective of this study involved the evaluation of two pre-evaporation internal and external chamber geometries. The geometry configuration should be able to achieve full evaporation of the low-grade palm oil before the fuel can be introduced to the main combustion chamber in vapor form. To achieve this target, exhaust gas recycling technique is implemented for both internal and external chamber designs to provide the needed heat for fuel evaporation. The performance of both geometries was evaluated based on the following criteria and response parameters:

i. Acceptable emission levels: Carbon monoxide (CO) <400ppm and Nitrogen oxide thermal (NOx) < 50ppm.
ii. Low TIT below 900°C to avoid damaging the turbine blades.
iii. Controlled flame propagation through the flame tube without flame leakage to the other undesired zones.
iv. Compactness, ease of fabrication and low cost.

Once the first objective is achieved, the chosen pre-evaporation chamber geometry coupled to the main chamber is then evaluated for the second objective. The evaluation involves comparing several geometries of the air inlet ducting and gas exhaust ducting. The evaluation criteria and response variables are similar to the criteria mentioned above with the addition of the hydrodynamic flow evaluation. This evaluation involves the flow velocity and pressure profiles. The ducting design should achieve smooth and homogeneous flow, avoiding low or high pressure pockets the can induce a swirling motion and cause flame disturbance and leakage.

The external pre-evaporation chamber geometry was fully optimized in our previous work [43] to achieve palm oil evaporation prior to the main MGT combustion chamber. The optimum geometry is connected in this study to the main combustion chamber and tested to evaluate the combustion of the low-grade palm oil as a fuel. An alternative method for the pre-evaporation of palm oil is also proposed in this work using internal pre-evaporation chamber. This internal chamber is based on a third internal annular tube (recycle tube) added to the conventional MGT combustion chamber that consists of outer air jacket and inner flame tube. At the top of this recycle tube, a row of (8 holes of 6 mm in diameter) was added to pass some of the exhaust hot gasses back to the chamber inlet. For the external pre-evaporation chamber, the recycle tube is extended through the chamber to preheat the fuel which is injected at the inlet of the pre-evaporation chamber. While for the internal pre-evaporation chamber, the fuel is injected at the chamber top and fuel droplets pass in parallel with the hot exhaust recycle gas which allows the internal pre-evaporation of the liquid fuel.

SOLIDWORKS software (2019) is used to draw the geometries of both chambers followed by the mesh creation in ANSYS work-bench. Figure 1 shows the drawings of the internal and external pre-evaporation chambers along with the main combustion chamber (core chamber). Fuel injection ports were not added physically to the chamber's geometry as the DPM model in ANSYS-Fluent CFD settings specifies the injection location for the liquid fuel droplets.

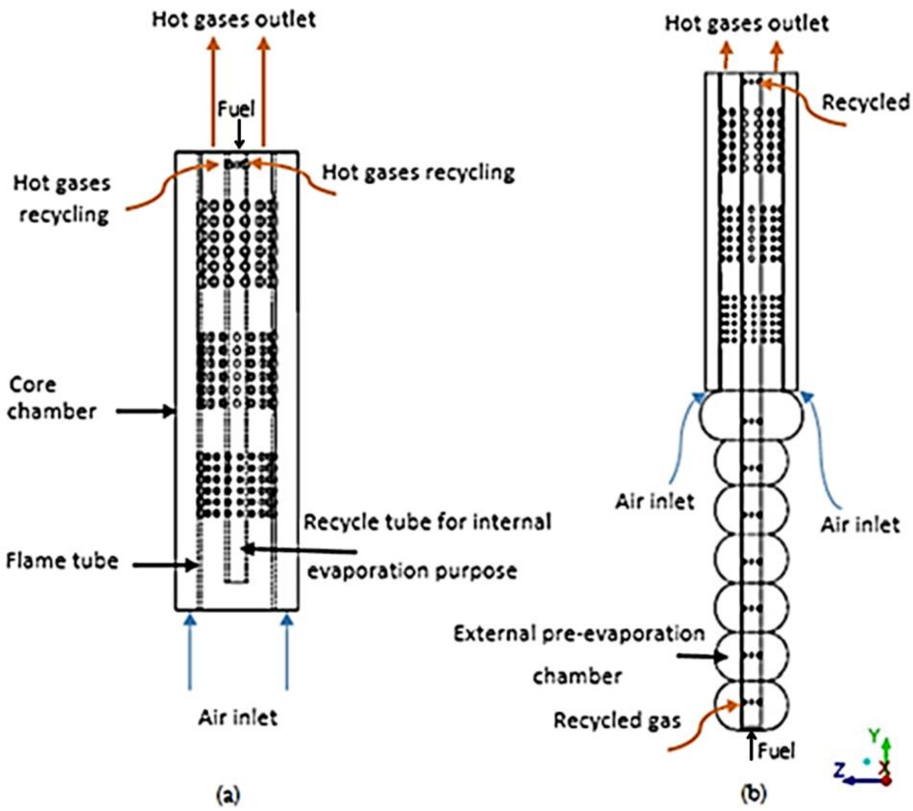

Fig. 1. Computational domains (a) Combustion chamber with internal recycle tube, (b) combustion chamber with external pre-evaporation chamber

Both geometry designs are then evaluated using CFD simulation based on the evaluation criteria mentioned before. The internal pre-evaporation chamber was chosen as will be discussed in the results. Thus, six geometries of the inlet and outlet ducting were proposed and added to the core chamber to allow smooth air entrance to the core chamber and exhaust exit from the chamber as shown in Figure 2.

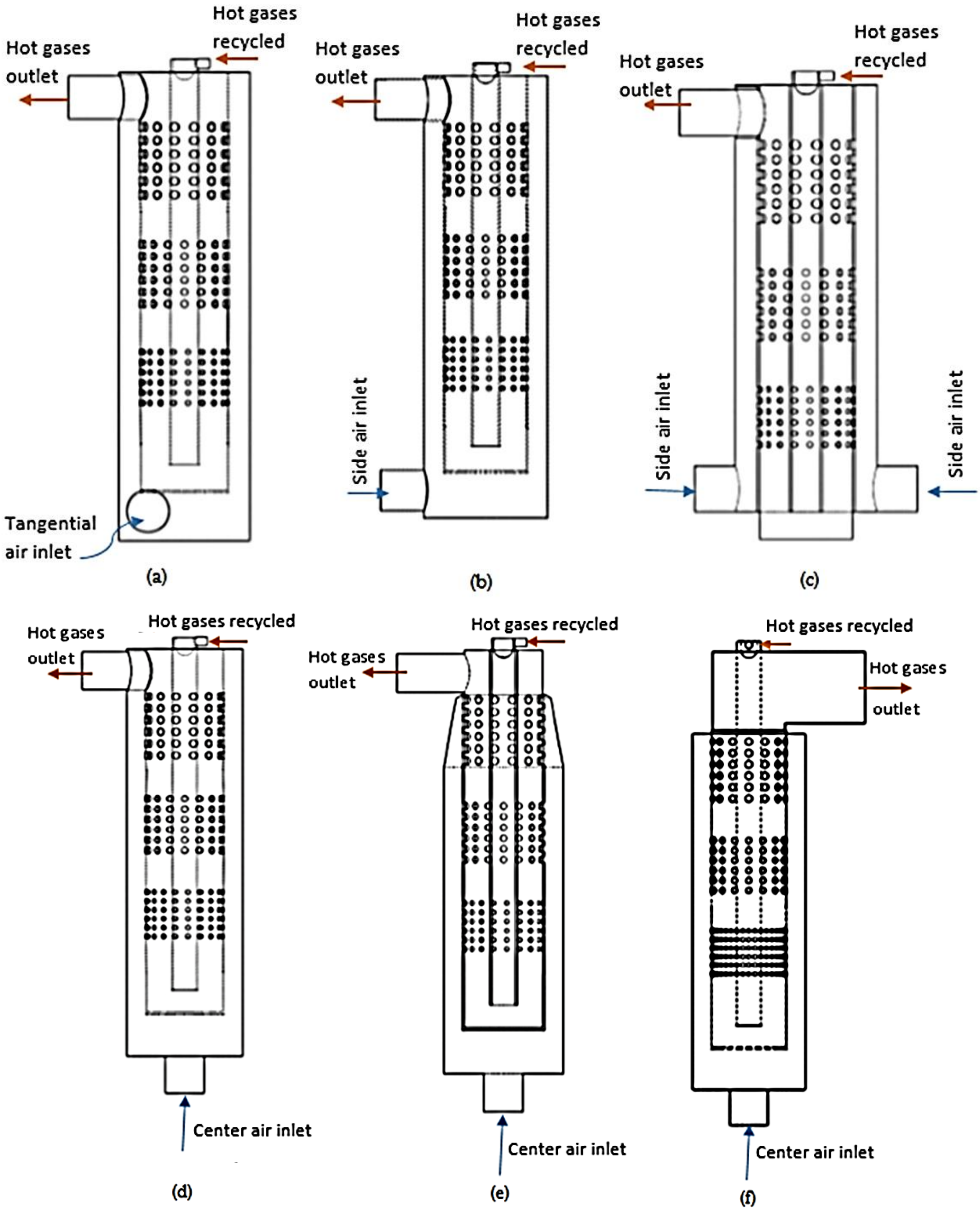

Fig. 2. Combustion chamber with (a) tangential air inlet and 90-degree gas outlet, (b) side air inlet and 90-degree gas outlet, (c) two side air inlets and 90-degree gas outlet, (d) centre air inlet and 90-degree gas outlet, (e) centre air inlet and 90-degree outlet with conical air jacket, (f) centre air inlet and 90-degree square ducting outlet

For the air inlet ducting, two designs were compared, involving side inlet design and centre (along the chamber axis) inlet design. For the side inlet design, tangential and non-tangential geometries are compared, in addition to single and multi-duct design. This wide variation of inlet geometries covers all the possible geometries, which allows the exploration of the effect of air inlet geometry on the performance of the core chamber. On the other hand, putting centre exhaust ducting along the axis of the chamber is not physically possible as the fuel injection is located at the chamber top at the centre. Therefore, only side exhaust ducting designs were tested involving circular and non-circular design. Single ducting was chosen to avoid any excessive insulation and heat loss.

2.3 CFD Simulation

ANSYS-Fluent software is used in order to analyzed the flow of recycle hot gas and simulate the flow of fuel inside chambers through the k-epsilon model. DPM is utilized to simulate the fuel injection and evaporation process while species transport model (mixture template) is used to identify the species of combustion process for both cases.

2.3.1 Species transport model

Species transport model is one of combustion model, the hypothesis in this model is complete combustion occurred and no CO emissions, so mixture model /eddy dissipation concept mechanism have been used and add a palm oil through Ansys fuel data base as $C_{55}H_{90.86}O_{1.51}N_{1.41}$ [47] .

2.3.2 DPM and viscosity model set-up

The k-ε model was used in this study since it suitable for flow with swirling motion. Heat transfer and turbulence behaviour can be predicted through standard k-ε model. This model is based on two transport equations for the turbulence kinetic energy (k) and its dissipation rate (ε) shown as Eq. (2) and Eq. (3), where, Gk and Gb are turbulence kinetic energy generation by mean velocity and buoyancy; YM is fluctuating dilatation contribution in compressible turbulence to the overall dissipation rate; C_1ε,C_2ε,C_3ε are constants; ρk,ρε are turbulent Prandtl numbers for k, ε. The heat losses through the outer walls were set as a fixed heat flux of 12.9 kW/m^2 calculated from the expected efficiency of this chamber. Discreet phase model (DPM) used to imitate the injection of fuel particles with 3 injectors. Three injector setups are arranged radially with 180° and 120° angle, respectively, between the injectors. Chamber axis is on X-axis, and the injection stream velocity for the Y & Z axes was changed from 0.6 m/s in the axis direction then drops to zero for the central stream then increases to 0.6 m/s in the opposite direction. Therefore, only the central injection stream travels parallel to the chamber axis while the two streams (on each side) are pushed tangentially towards Y & Z axes creating a swirl injector motion with 30° injector angle to match the specification of the commercially available fuel injectors that will be used in the experimental phase of this project. The boundary conditions of the pre-evaporation chamber and DPM injector setup for three injector mode with multiple droplets set for outer pre-evaporation chamber is shown in Table 2. There is no fuel inlet boundary condition since the fuel injection is handled by the DPM.

$$\frac{\partial}{\partial t}(\rho k)+\frac{\partial}{\partial x_i}(\rho k u_{i)}=\frac{\partial}{\partial x_j}\left[\left(u+\frac{u_t}{\partial_k}\right)\frac{\partial k}{\partial x_j}\right]+G_k+G_b-\rho\varepsilon-Y_M+S_k \quad (2)$$

$$\frac{\partial}{\partial t}(\rho \varepsilon)+\frac{\partial}{\partial x_i}(\rho \varepsilon u_{i)}=\frac{\partial}{\partial x_j}\left[\left(u+\frac{u_t}{\partial_\varepsilon}\right)\frac{\partial \varepsilon}{\partial x_j}\right]+C_{1\varepsilon}\frac{\varepsilon}{k}(G_k+C_{3\varepsilon}G_b)-C_{2\varepsilon}\rho\frac{\varepsilon^2}{k}+S_\varepsilon \quad (3)$$

Table 2
DPM 3-injectors setup

Injection type	Group
Particle type	Droplet
Number of streams	5
Temperature/K	300
Flow rate per stream (kg/s)	0.000174
X-velocity (m/s)	1
Y-velocity (m/s)	+0.6 to -0.6
Z-velocity (m/s)	+0.6 to -0.6

The boundary condition for the main combustion chamber with interior fuel evaporation and for chamber connected with external pre-evaporation chamber was set as in Table 3. Thermal losses from walls (in the form of heat flux) are calculated based on 90% chamber efficiency, in reference to fuel input.

Table 3
Boundary conditions

Parameters	Value
Fuel inlet	
Temperature/K	473
Pressure/bar	1
Air inlet	
Temperature/K	431
Pressure/bar	1
Mass flow rate/(kg/s)	0.08210698
Outlet	
Pressure/bar	1
Back flow temperature/K	1000
Inner walls	
Materials	steel
Outer walls	
Materials	steel
Wall thickness/mm	6
Heat fluxes/(w/m^2)	-12946

While DPM injector set up for the main combustion chamber with interior evaporation tube are tabulated in Table 4.

Table 4
DPM main combustion chamber

Injection type	Group
Particle type	Droplet
Number of streams	5
Temperature/K	300
Flow rate per stream (kg/s)	0.000524
X-velocity (m/s)	1
Y-velocity (m/s)	+0.6 to -0.6
Z-velocity (m/s)	+0.6 to -0.6

3. Results and Discussion

3.1 Comparison between Pre-Evaporation External Chamber and Internal Recycle Tube

Figure 3 shows the temperature and emission (CO and NOx) profiles obtained from the CFD simulation of palm oil combustion in MGT combustor with internal pre-evaporation chamber. Results showed good flame and temperature distribution along the flame tube which indicated that the chamber followed the design characteristics regarding air distribution and air fuel ratio. This can be observed from the combustion behaviour, which was rich near premix zone followed by stoichiometric behaviour in combustion zone and ended by dilution zone at chamber exit with low CO concentration about 243 ppm. Combustion intensity increased between the pre-mix and combustion zones resulting in high temperature elevation up to 2500K. This resulted in thermal NOx formation at that zone as can be observed from NOx profile, while the formation reduced downstream due to the cooling effect of dilution air. NOx showed acceptable value of 37.9 ppm at the chamber exit, with acceptable TIT value of about 899°C. CO emission profile provided good insight of the fuel pre-evaporation and the progress of the combustion. It can be noticed that no combustion occurred inside the recycle tube (as indicated by the lack of CO), where palm oil droplets gradually evaporated along the tube with no oxidizer to start the flame. Once the fuel vapor exited the recycle tube (at the flame tube bottom), the high temperature causes the vapor devolatilization and partial oxidation which accelerated the generation of CO. The concentration of CO dropped drastically at the hot combustion zone indicating the full oxidation of CO into CO_2. CO concentration kept dropping towards the chamber exit, where the only traces of CO gas could be seen near the centre of the flame tube, far from the air supply.

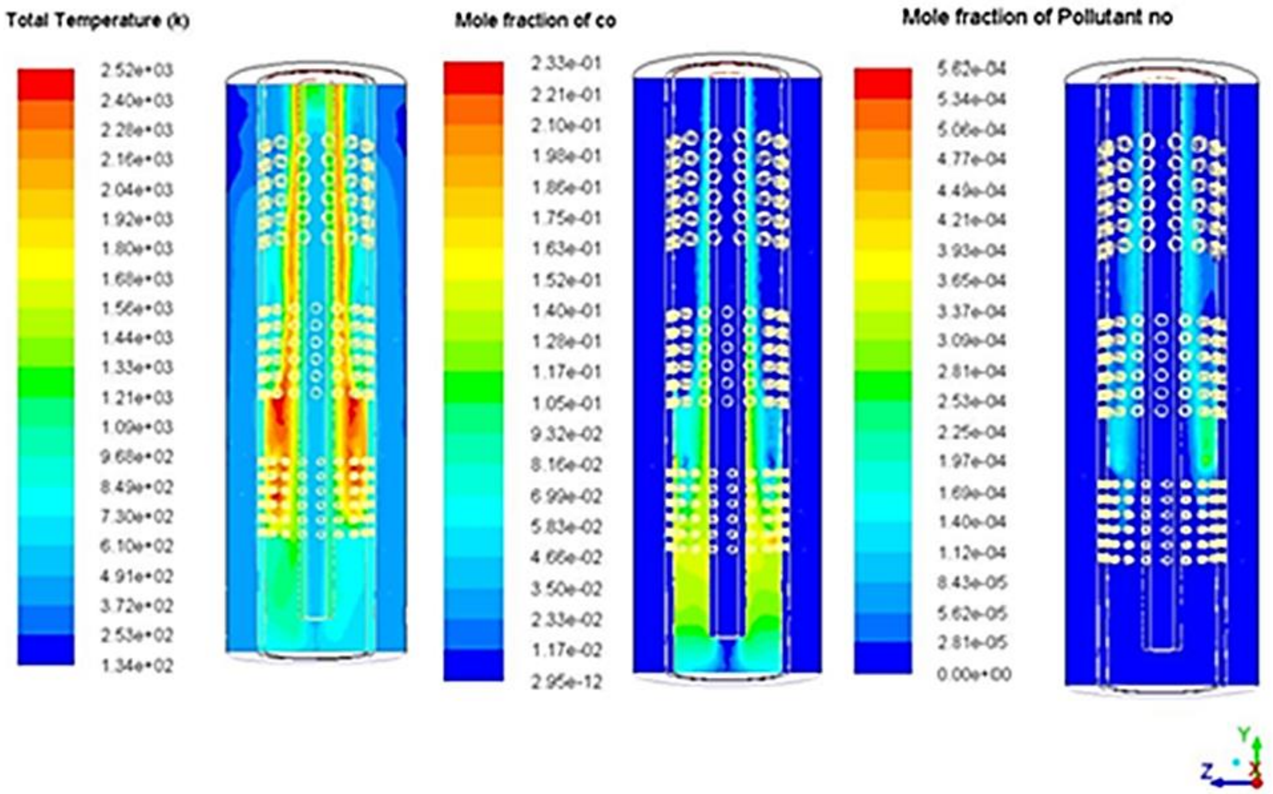

Fig. 3. Chamber with internal recycle tube

Figure 4 shows the contours of temperature, CO and NOx for the MGT combustion chamber along with the external pre-evaporation chamber. The flame was not distributed homogenously compared to the internal pre-evaporation chamber design. This could be attributed to the geometry of the pre-evaporation chamber which is based on an outer wall with revolves that creates swirling motion and eddies. CO contours showed that the fuel droplets were adequately evaporated and devolatilization and partial oxidation of the fuel started early before the exit of the pre-evaporation chamber. The flame started inside the last revolve of the pre-evaporation chamber due to the sudden expansion in volume which caused a drop in flow velocity that sustained flame start-up. The flame was disturbed and not evenly distributed inside the flame tube due to the swirling motion from the revolves geometry. Part of the flame was pushed inside the recycle tube which is not desirable as it will cause high material corrosion and degradation due to the elevated temperature with no air cooling, which will shorten the lifespan of the chamber. The flame tube zones did not function as intended to control the flame; however, the extended length of the tube was adequate to achieve complete combustion with low CO emissions of 183 ppm at the chamber exit. Also, thermal NOx generation was mostly concentrated at the hot zone where the flame started at the exit of the pre-evaporation chamber, resulting in low NOx emission of 25 ppm at the chamber exit. TIT was lower of about 800°C for this design as the flame was pulled down by the pre-evaporation chamber. Despite having lower TIT and emissions from this design, the chamber design with internal pre-evaporation still achieved acceptable results and was chosen from the manufacturing point of view, as the chamber with external pre-evaporation was too long compared to the core chamber which make it more costly and difficult to manufacture and fix within the MGT mounting frame. Besides that, it will need extensive insulation to maintain the hot recycle gas temperature passing from the main chamber to pre-evaporation chamber. On the other hand, the chamber with internal evaporation and gas recycling is insulated with the outer air jacket which recycles the heat back to the chamber with minimal heat losses.

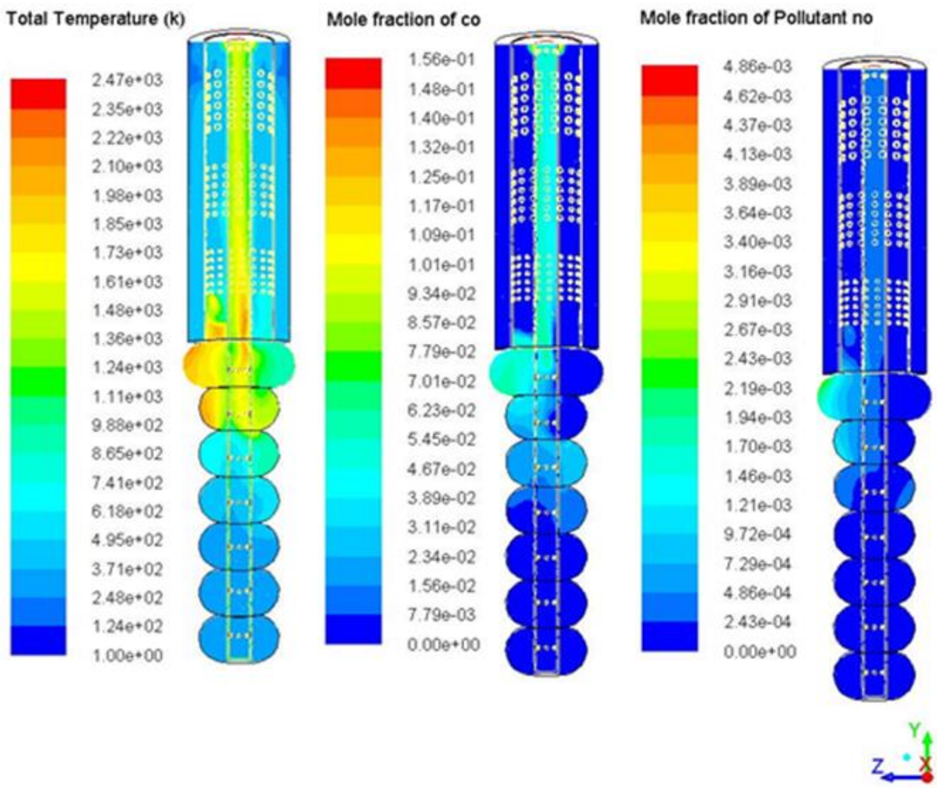

Fig. 4. Chamber with external pre-evaporation chamber

3.2 Air Inlet and Hot Gases Exhaust Ports

The chamber with internal fuel pre-evaporation was selected in the previous section as the optimum geometry. The ducting for air inlet and hot gases exhaust should be designed to be linked to the chamber to be ready to be assembled with the main test rig frame in the laboratory. Six configurations with centre, side and tangential air inlet duct geometries along with the exhaust gas duct configurations with 90-degree angle were shown earlier in the methodology section. Additionally, an exhaust gas recycling port was added to the recycle tube top to insure consistent flow of exhaust (5% of exhaust gas). This eliminates any effect of exhaust gas flow fluctuation that can be caused by the exhaust duct geometry, in order to maintain the ducts geometry as the only variable in this evaluation while all other factors are kept as constants for accurate evaluation of the duct geometry effect on combustion. Temperature, pressure and velocity contours from CFD simulation are shown in Figure 5.

Also, to fully evaluate the combustion performance for the different ducting geometries, the temperature at the chamber exit (TIT) along with CO emissions were recorded, as shown in Figure 6. First tested geometry included tangential air inlet with regular circular 90-degree gas exhaust port, shown in Figure 5(a). A centrifugal effect generated by the tangential air inlet geometry resulted in flame disturbance and bleeding out of the flame tube. The flow disturbance was indicated by the fluctuation in the flow velocity and pressure at the outer air jacket. This in turn caused inefficient air-fuel mixing at the different zones leading to incomplete combustion as indicated by the high CO emission of about 1300 ppm. The other issue is the unsymmetrical flow of exhaust gas as the gas is pushed upwards due to the 90-degree bend. The problem of the centrifugal effect caused by the tangential inlet can be solved by proposing a non-tangential side inlet port as shown in Figure 5(b). This configuration showed a non-symmetric flame around flame tube because the air flow compression effect towards the air jacket in the opposite side of the inlet. This also caused flame disturbance inside the flame tube, where the flame was pushed to one side, which caused slight elevation in CO emissions above 600 ppm. The exhaust gas flow issue was also obvious here due to the sharp bend with a limited duct diameter of 50mm. Adding one more air inlet duct in the opposite direction solved the problem of flame homogeneity inside flame tube as shown in Figure 5(c). However, this did not fully solve the flame bleeding issue as the slight elevation in air pressure around the pre-mix zone pushed the flame outwards at the combustion zone. This elevated CO emission to about 560 ppm. Also, having two inlet ducts is not preferable due to the added complexity and cost. Therefore, the air jacket was extended slightly downwards to allow the addition of a centre air inlet duct aligned with the chamber axis as shown in Figure 5(d). This configuration showed better symmetrical flow inside flame tube compared to the previous geometry. CO emissions dropped to slightly above 400 ppm, however, slight flame bleeding can still be observed. The exhaust duct in this configuration passed through the air jacket on one side only, which could cause air flow disturbance at the chamber top at dilution zone. Therefore, the air jacket at exhaust side was tapered to a conical shape before reaching the exhaust port, which provides symmetric air flow to the dilution zone as shown in Figure 5(e). Unexpectedly, the conical air jacket geometry performed poorly with a degraded combustion stability causing high elevation of CO emissions above 1100 ppm, which could be caused by the sudden increase in pressure at dilution zone which pushed the flame towards the air jacket. Therefore, the conical air jacket geometry was removed, and the last configuration shown in Figure 5(f) represents the optimum configuration with one centre air inlet duct and a large square duct at the exhaust. Increasing the height of the exhaust duct from 50mm to 100mm reduced the negative effect of the 90-degree change in flow direction and eliminated the back-pressure effect on one side of the flame tube.

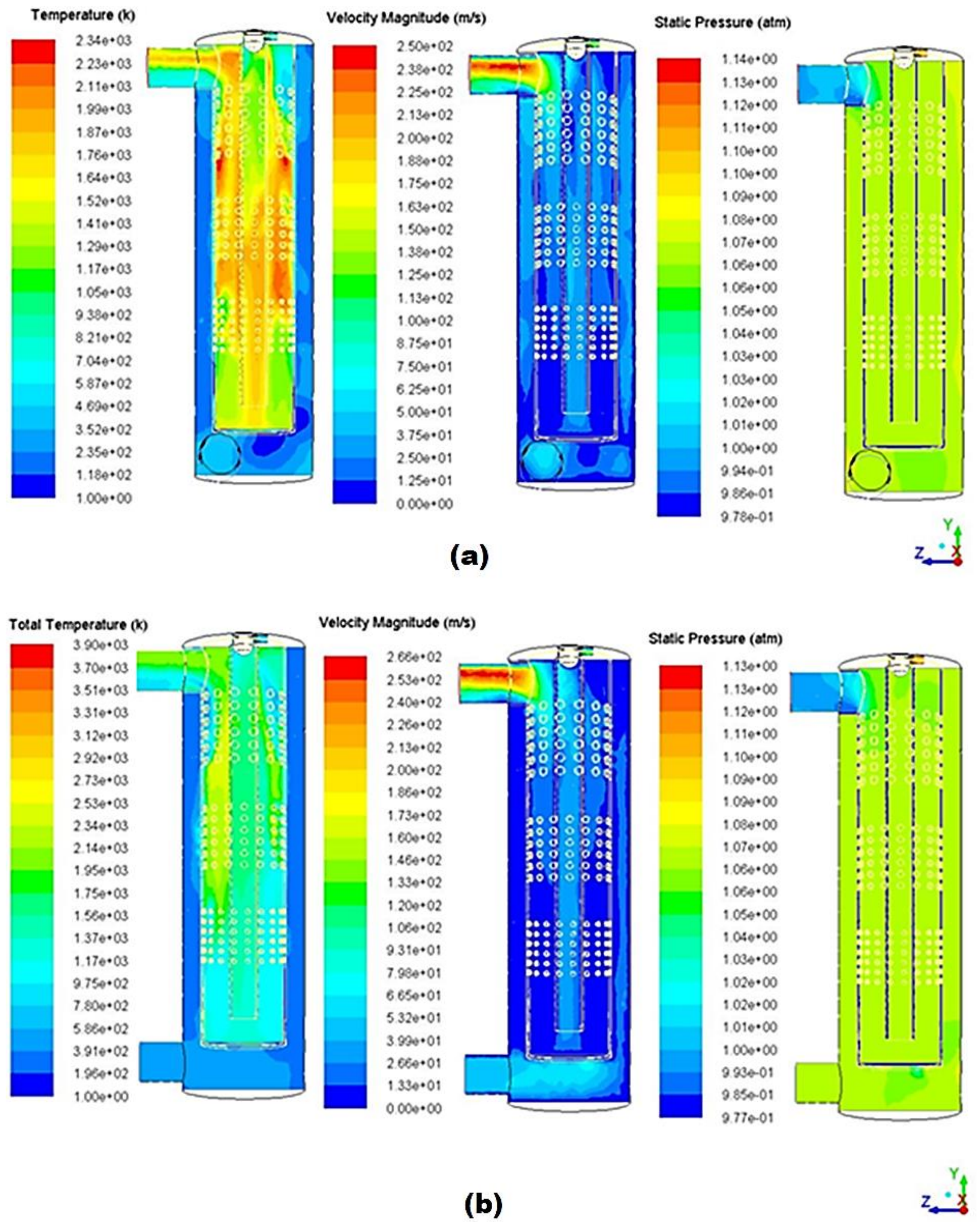
Temperature (k)
2.34e+03
2.23e+03
2.11e+03
1.99e+03
1.87e+03
1.76e+03
1.64e+03
1.52e+03
1.41e+03
1.29e+03
1.17e+03
1.05e+03
9.38e+02
8.21e+02
7.04e+02
5.87e+02
4.69e+02
3.52e+02
2.35e+02
1.18e+02
1.00e+00
Velocity Magnitude (m/s)
2.50e+02
2.38e+02
2.25e+02
2.13e+02
2.00e+02
1.88e+02
1.75e+02
1.63e+02
1.50e+02
1.38e+02
1.25e+02
1.13e+02
1.00e+02
8.75e+01
7.50e+01
6.25e+01
5.00e+01
3.75e+01
2.50e+01
1.25e+01
0.00e+00
Static Pressure (atm)
1.14e+00
1.13e+00
1.12e+00
1.11e+00
1.10e+00
1.10e+00
1.09e+00
1.08e+00
1.07e+00
1.06e+00
1.06e+00
1.05e+00
1.04e+00
1.03e+00
1.03e+00
1.02e+00
1.01e+00
1.00e+00
9.94e-01
9.86e-01
9.78e-01
Y
Z
X
(a)
Total Temperature (k)
3.90e+03
3.70e+03
3.51e+03
3.31e+03
3.12e+03
2.92e+03
2.73e+03
2.53e+03
2.34e+03
2.14e+03
1.95e+03
1.75e+03
1.56e+03
1.37e+03
1.17e+03
9.75e+02
7.80e+02
5.86e+02
3.91e+02
1.96e+02
1.00e+00
Velocity Magnitude (m/s)
2.66e+02
2.53e+02
2.40e+02
2.26e+02
2.13e+02
2.00e+02
1.86e+02
1.73e+02
1.60e+02
1.46e+02
1.33e+02
1.20e+02
1.06e+02
9.31e+01
7.98e+01
6.65e+01
5.32e+01
3.99e+01
2.66e+01
1.33e+01
0.00e+00
Static Pressure (atm)
1.13e+00
1.13e+00
1.12e+00
1.11e+00
1.10e+00
1.09e+00
1.09e+00
1.08e+00
1.07e+00
1.06e+00
1.06e+00
1.05e+00
1.04e+00
1.03e+00
1.02e+00
1.02e+00
1.01e+00
1.00e+00
9.93e-01
9.85e-01
9.77e-01
Y
Z
X
(b)

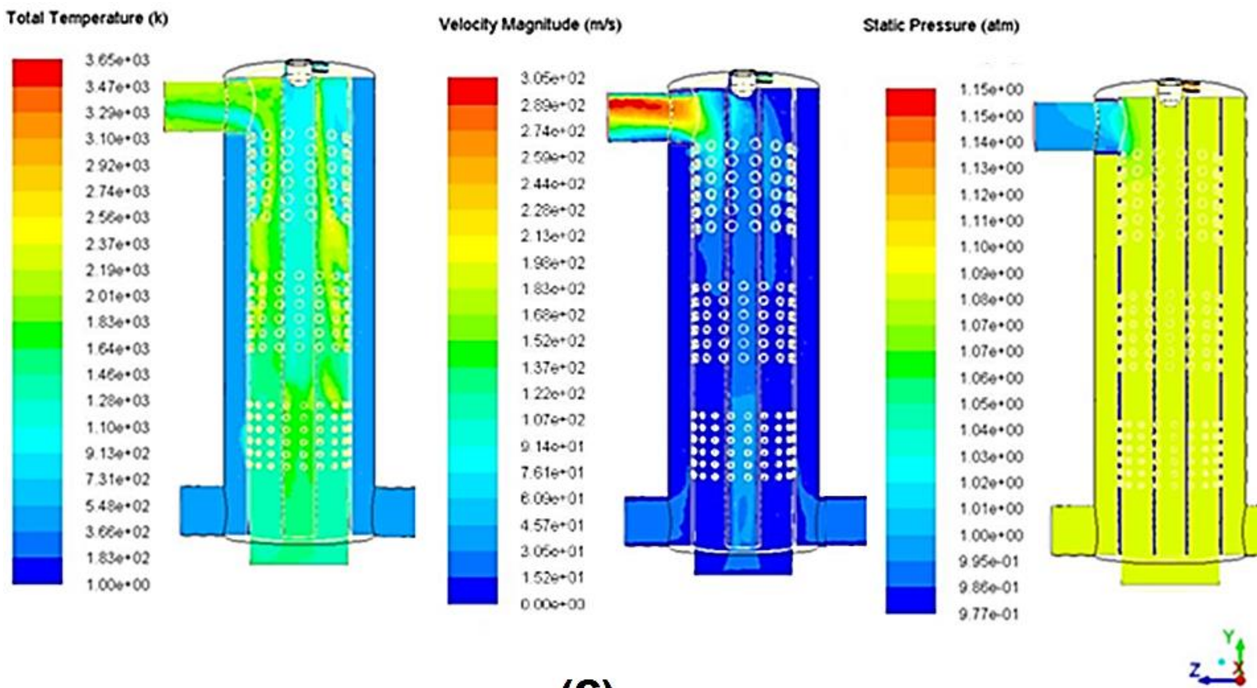
Total Temperature (k)
3.65e+03
3.47e+03
3.29e+03
3.10e+03
2.92e+03
2.74e+03
2.56e+03
2.37e+03
2.19e+03
2.01e+03
1.83e+03
1.64e+03
1.46e+03
1.28e+03
1.10e+03
9.13e+02
7.31e+02
5.48e+02
3.66e+02
1.83e+02
1.00e+00
Velocity Magnitude (m/s)
3.05e+02
2.89e+02
2.74e+02
2.59e+02
2.44e+02
2.28e+02
2.13e+02
1.98e+02
1.83e+02
1.68e+02
1.52e+02
1.37e+02
1.22e+02
1.07e+02
9.14e+01
7.61e+01
6.09e+01
4.57e+01
3.05e+01
1.52e+01
0.00e+00
Static Pressure (atm)
1.15e+00
1.15e+00
1.14e+00
1.13e+00
1.12e+00
1.11e+00
1.10e+00
1.09e+00
1.08e+00
1.07e+00
1.07e+00
1.06e+00
1.05e+00
1.04e+00
1.03e+00
1.02e+00
1.01e+00
1.00e+00
9.95e-01
9.86e-01
9.77e-01
Y
Z
X

(c)

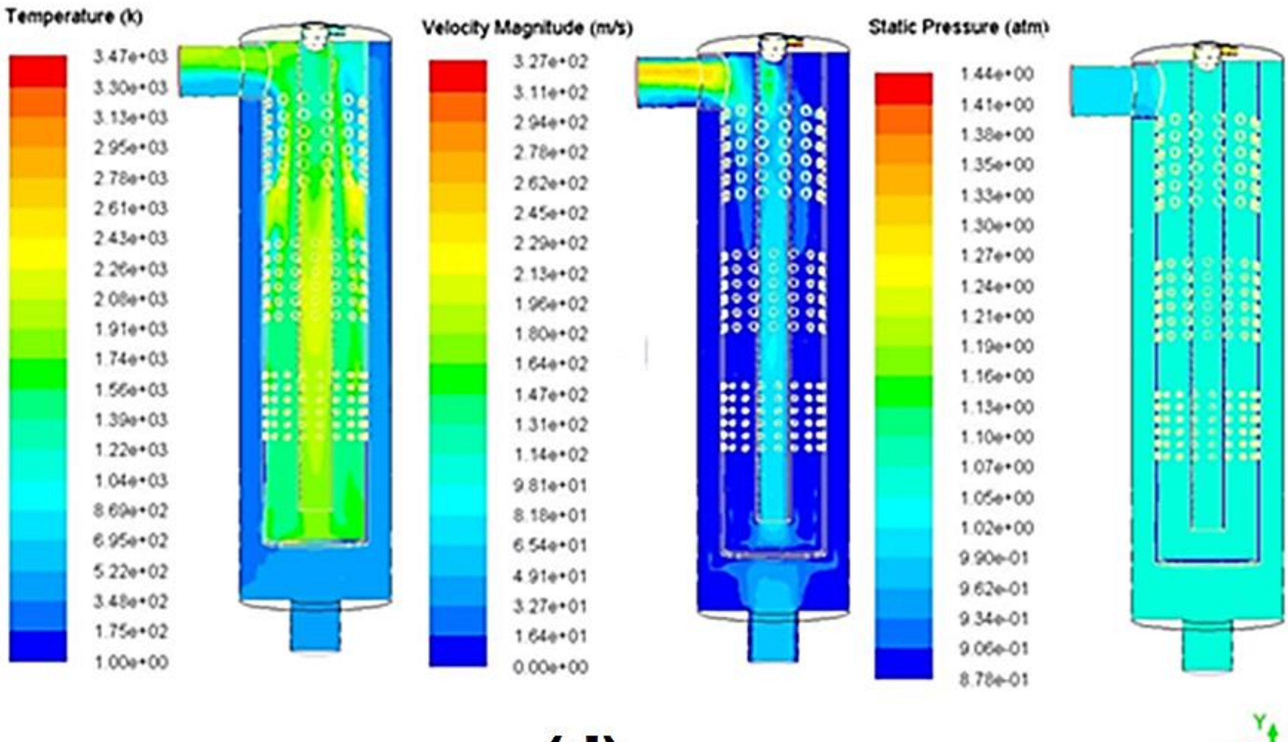
Temperature (k)
3.47e+03
3.30e+03
3.13e+03
2.95e+03
2.78e+03
2.61e+03
2.43e+03
2.26e+03
2.08e+03
1.91e+03
1.74e+03
1.56e+03
1.39e+03
1.22e+03
1.04e+03
8.69e+02
6.95e+02
5.22e+02
3.48e+02
1.75e+02
1.00e+00
Velocity Magnitude (m/s)
3.27e+02
3.11e+02
2.94e+02
2.78e+02
2.62e+02
2.45e+02
2.29e+02
2.13e+02
1.96e+02
1.80e+02
1.64e+02
1.47e+02
1.31e+02
1.14e+02
9.81e+01
8.18e+01
6.54e+01
4.91e+01
3.27e+01
1.64e+01
0.00e+00
Static Pressure (atm)
1.44e+00
1.41e+00
1.38e+00
1.35e+00
1.33e+00
1.30e+00
1.27e+00
1.24e+00
1.21e+00
1.19e+00
1.16e+00
1.13e+00
1.10e+00
1.07e+00
1.05e+00
1.02e+00
9.90e-01
9.62e-01
9.34e-01
9.06e-01
8.78e-01
Y
Z
X

(d)

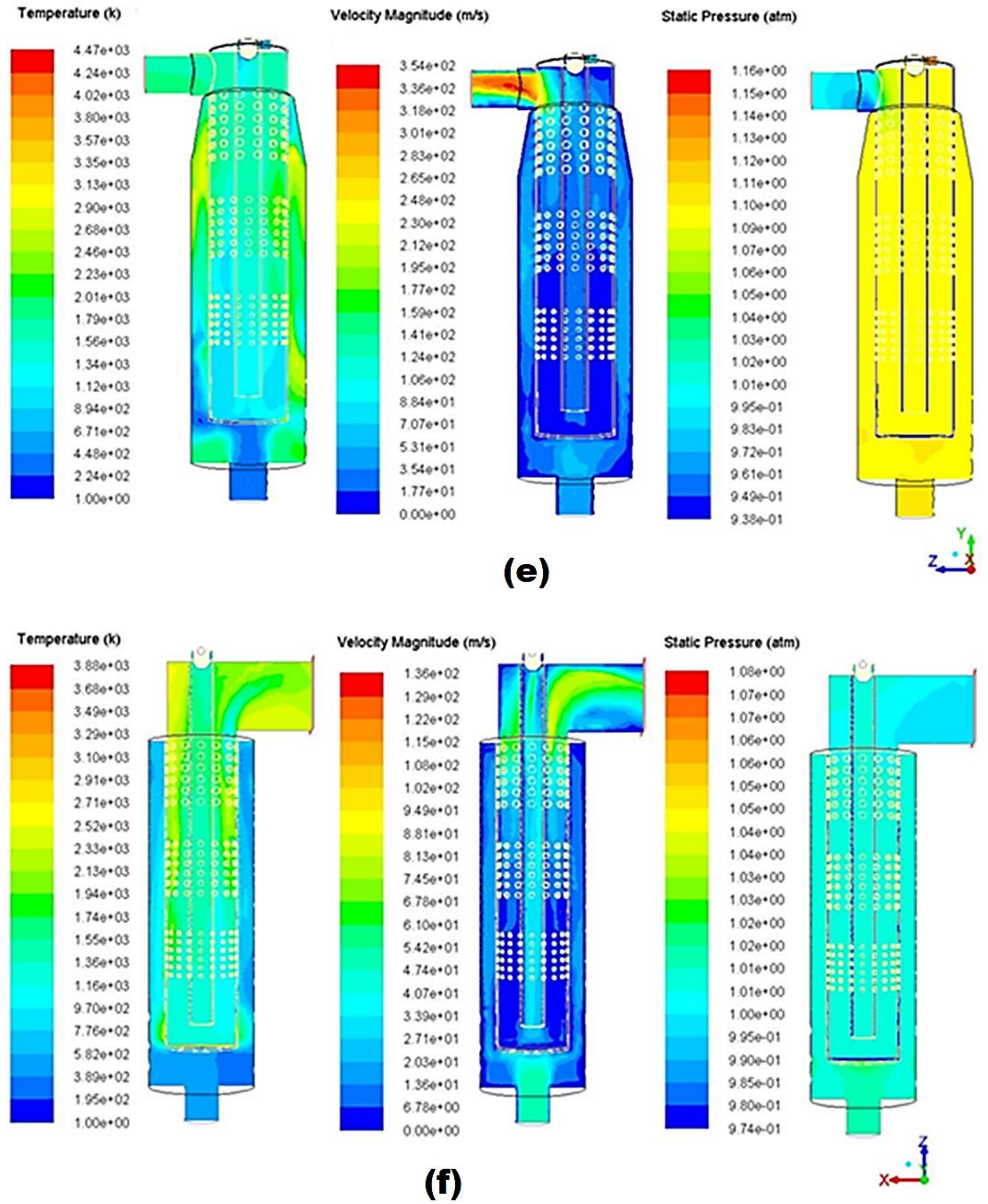

Fig. 5. Combustion chamber with different air inlet and gases exhaust contours

This solved the flame bleeding issue and restored flame homogeneity inside flame tube and inside exhaust port. This geometry achieved the lowest CO emission of 312 ppm among the 6 geometries as shown in Figure 6.

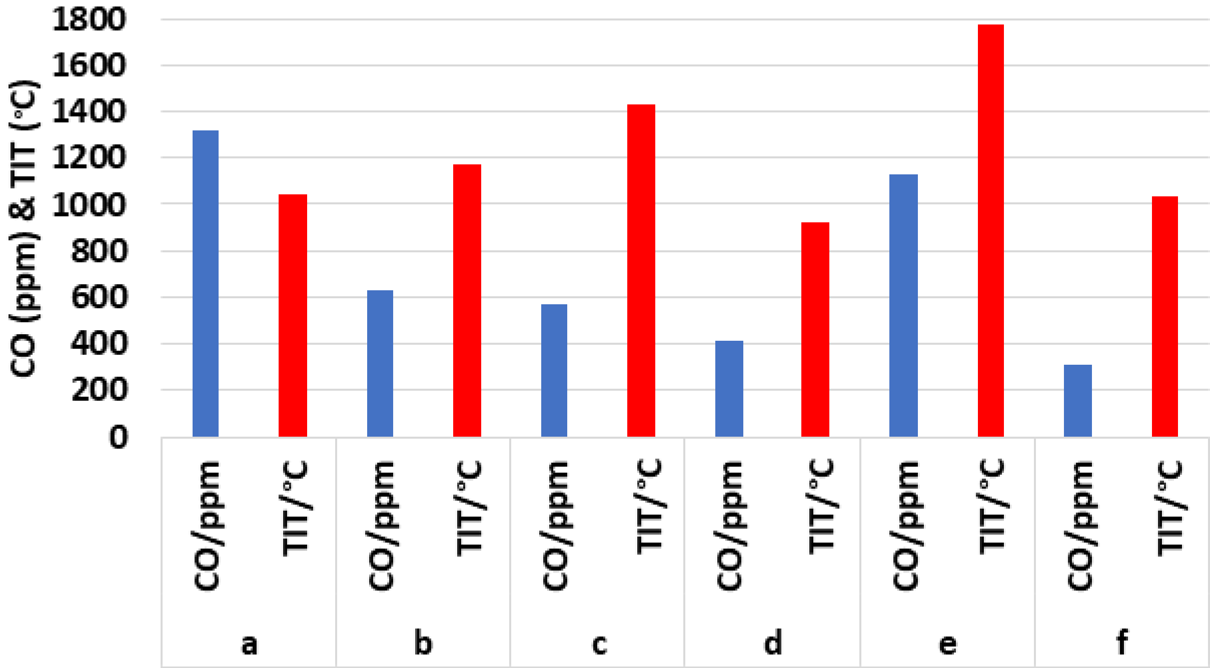

Fig. 6. Comparison between 6 different air inlet and hot gas exhaust configurations

4. Conclusions

In this study, a new MGT combustion chamber geometry with three annular-tube design was evaluated for the combustion of low-grade biofuels. Exhaust gas recycling technique was implemented for the evaporation of liquid biofuels where the recycled gas is passed through the inner annular tube. Two different approaches were taken into consideration using external and internal pre-evaporation chambers. Having a dedicated external chamber for the fuel evaporation achieved complete evaporation prior to the main chamber which prompted early start of the flame. This provided lower CO emission and TIT compared to the other design. However, utilizing the inner annular tube as the pre-evaporation chamber by passing the hot exhaust recycled gas along with the liquid fuel spray provided a simpler design while maintaining a compact chamber design with lower cost and acceptable TIT and emissions. Therefore, from the economical and manufacturing point of view, the internal pre-evaporation chamber was chosen for this design. The next stage towards a complete MGT combustion chamber design was to optimize the air inlet and exhaust ducting the will be connected to the core chamber. Therefore, 8 inlet and outlet ducting designs were compared in terms of the flow hydrodynamics, flame stability, TIT and CO emissions. It was observed that the flame inside the flame tube was sensitive to any disturbance in air flow in the air jacket, due to the limited gap between the flame tube and outer jacket, which is the case for most common MGT combustion chamber designs. Therefore, any non-symmetric air flaw in the jacket due to the swirling flow caused by tangential inlet, or the non-axial flow caused by side inlet will cause flame disturbance and bleeding out of the flame tube. To overcome this issue, the air stream has to be parallel to the axis of the chamber. Similarly, having a side exhaust duct on 90-degree angle to the axis chamber caused a similar issue, but increasing the duct size mitigated the negative effect.

Acknowledgement
The authors would like to thank the Ministry of Education Malaysia, Fundamental Research Grant Scheme (FRGS) 203.PMEKANIK.6071426, project ID: 13731, Reference Code: FRGS/1/2019/TK07/USM/02/2, for the financial support of this study.

References
[1] Samsudin, Muhammad Syazwan Nizam, Md Mizanur Rahman, and Muhamad Azhari Wahid. "Sustainable power generation pathways in Malaysia: Development of long-range scenarios." *Journal of Advanced Research in Applied Mechanics* 24, no. 1 (2016): 22-38.
[2] Hudda, Neelakshi, Liam W. Durant, Scott A. Fruin, and John L. Durant. "Impacts of aviation emissions on near-airport residential air quality." *Environmental Science & Technology* 54, no. 14 (2020): 8580-8588. https://doi.org/10.1021/acs.est.0c01859
[3] Grobler, Carla, Philip J. Wolfe, Kingshuk Dasadhikari, Irene C. Dedoussi, Florian Allroggen, Raymond L. Speth, Sebastian D. Eastham *et al.,* "Marginal climate and air quality costs of aviation emissions." *Environmental Research Letters* 14, no. 11 (2019): 114031. https://doi.org/10.1088/1748-9326/ab4942
[4] Nicolini, Marcella, and Massimo Tavoni. "Are renewable energy subsidies effective? Evidence from Europe." *Renewable and Sustainable Energy Reviews* 74 (2017): 412-423. https://doi.org/10.1016/j.rser.2016.12.032
[5] Yacob, Noraishah Shafiqah, and Hassan Mohamed. "Investigation of palm oil wastes characteristics for co-firing with coal." *Journal of Advanced Research in Applied Sciences and Engineering Technology* 23, no. 1 (2021): 34-42. https://doi.org/10.37934/araset.23.1.3442
[6] Colak, Ilhami, Seref Sagiroglu, Mehmet Demirtas, and Mehmet Yesilbudak. "A data mining approach: Analyzing wind speed and insolation period data in Turkey for installations of wind and solar power plants." *Energy Conversion and Management* 65 (2013): 185-197. https://doi.org/10.1016/j.enconman.2012.07.011
[7] Zhou, Cheng, Elham Doroodchi, and Behdad Moghtaderi. "An in-depth assessment of hybrid solar–geothermal power generation." *Energy conversion and management* 74 (2013): 88-101. https://doi.org/10.1016/j.enconman.2013.05.014
[8] Islam, Md Tasbirul, S. A. Shahir, TM Iftakhar Uddin, and A. Z. A. Saifullah. "Current energy scenario and future prospect of renewable energy in Bangladesh." *Renewable and Sustainable Energy Reviews* 39 (2014): 1074-1088. https://doi.org/10.1016/j.rser.2014.07.149
[9] Demirbas, Ayhan. "Waste management, waste resource facilities and waste conversion processes." *Energy Conversion and Management* 52, no. 2 (2011): 1280-1287. https://doi.org/10.1016/j.enconman.2010.09.025
[10] Corro, Grisel, Laura Paniagua, Umapada Pal, Fortino Bañuelos, and Minerva Rosas. "Generation of biogas from coffee-pulp and cow-dung co-digestion: Infrared studies of postcombustion emissions." *Energy conversión and Management* 74 (2013): 471-481. https://doi.org/10.1016/j.enconman.2013.07.017
[11] Khalil, Ahmed EE, and Ashwani K. Gupta. "Clean combustion in gas turbine engines using Butyl Nonanoate biofuel." *Fuel* 116 (2014): 522-528. https://doi.org/10.1016/j.fuel.2013.08.022
[12] Yacob, Noraishah Shafiqah, and Hassan Mohamed. "Investigation of palm oil wastes characteristics for co-firing with coal." *Journal of Advanced Research in Applied Sciences and Engineering Technology* 23, no. 1 (2021): 34-42. https://doi.org/10.37934/araset.23.1.3442
[13] Sundararaj, Ramraj H., Roshan Dinesh Kumar, Anoop Kumar Raut, T. Chandra Sekar, Vivek Pandey, Abhijit Kushari, and S. K. Puri. "Combustion and emission characteristics from biojet fuel blends in a gas turbine combustor." *Energy* 182 (2019): 689-705. https://doi.org/10.1016/j.energy.2019.06.060
[14] Boomadevi, P., V. Paulson, Stanley Samlal, Madhanraj Varatharajan, Manigandan Sekar, Mishal Alsehli, Ashraf Elfasakhany, and Siriporn Tola. "Impact of microalgae biofuel on microgas turbine aviation engine: A combustion and emission study." *Fuel* 302 (2021): 121155. https://doi.org/10.1016/j.fuel.2021.121155
[15] Ye, Jingjing, Paul R. Medwell, Emilien Varea, Stephan Kruse, Bassam B. Dally, and Heinz G. Pitsch. "An experimental study on MILD combustion of prevaporised liquid fuels." *Applied Energy* 151 (2015): 93-101. https://doi.org/10.1016/j.apenergy.2015.04.019
[16] Reddy, V. Mahendra, and Sudarshan Kumar. "Development of high intensity low emission combustor for achieving flameless combustion of liquid fuels." *Propulsion and Power Research* 2, no. 2 (2013): 139-147. https://doi.org/10.1016/j.jppr.2013.04.006
[17] Reddy, V. Mahendra, Amit Katoch, William L. Roberts, and Sudarshan Kumar. "Experimental and numerical analysis for high intensity swirl based ultra-low emission flameless combustor operating with liquid fuels." *Proceedings of the Combustion Institute* 35, no. 3 (2015): 3581-3589. https://doi.org/10.1016/j.proci.2014.05.070

[18] Rahman, Nik Kechik Mujahidah Nik Abdul, Syamimi Saadon, and Mohd Hasrizam Che Man. "Heat Transfer Enhancement of Biomass Based Stirling Engine." *Journal of Advanced Research in Fluid Mechanics and Thermal Sciences* 100, no. 1 (2022): 1-10. https://doi.org/10.37934/arfmts.100.1.110

[19] Hashimoto, Nozomu, Yasushi Ozawa, Noriyuki Mori, Isao Yuri, and Tohru Hisamatsu. "Fundamental combustion characteristics of palm methyl ester (PME) as alternative fuel for gas turbines." *Fuel* 87, no. 15-16 (2008): 3373-3378. https://doi.org/10.1016/j.fuel.2008.06.005

[20] Kurji, Hayder, Agustin Valera-Medina, Jon Runyon, Anthony Giles, Daniel Pugh, Richard Marsh, N. Cerone, F. Zimbardi, and V. Valerio. "Combustion characteristics of biodiesel saturated with pyrolysis oil for power generation in gas turbines." *Renewable Energy* 99 (2016): 443-451. https://doi.org/10.1016/j.renene.2016.07.036

[21] Suchocki, Tomasz, P. Lampart, P. Kazimierski, K. Januszewicz, and B. Gawron. "Experimental investigation of performance and emission characteristics of a miniature gas turbine supplied by blends of kerosene and waste tyre pyrolysis oil." *Energy* 215 (2021): 119125. https://doi.org/10.1016/j.energy.2020.119125

[22] Seljak, T., and T. Katrašnik. "Emission reduction through highly oxygenated viscous biofuels: use of glycerol in a micro gas turbine." *Energy* 169 (2019): 1000-1011. https://doi.org/10.1016/j.energy.2018.12.095

[23] Enagi, Ibrahim I., K. A. Al-Attab, and Z. A. Zainal. "Combustion chamber design and performance for micro gas turbine application." *Fuel processing technology* 166 (2017): 258-268. https://doi.org/10.1016/j.fuproc.2017.05.037

[24] Enagi, Ibrahim I., Khaled A. Al-attab, and Zainal Alimuddin Zainal. "Liquid fuels spray and combustion characteristics in a new micro gas turbine combustion chamber design." *International Journal of Energy Research* 43, no. 8 (2019): 3365-3380. https://doi.org/10.1002/er.4475

[25] Zhao, Zhen-yu, Hong Yan, Jian Zuo, Yu-xi Tian, and George Zillante. "A critical review of factors affecting the wind power generation industry in China." *Renewable and Sustainable Energy Reviews* 19 (2013): 499-508. https://doi.org/10.1016/j.rser.2012.11.066

[26] Das, Mithun, Mouktik Sarkar, Amitava Datta, and Apurba Kumar Santra. "An experimental study on the combustion, performance and emission characteristics of a diesel engine fuelled with diesel-castor oil biodiesel blends." *Renewable Energy* 119 (2018): 174-184. https://doi.org/10.1016/j.renene.2017.12.014

[27] Hallett, W. L. H., and N. V. Legault. "Modelling biodiesel droplet evaporation using continuous thermodynamics." *Fuel* 90, no. 3 (2011): 1221-1228. https://doi.org/10.1016/j.fuel.2010.11.035

[28] Raghuwanshi, Sanjeev, Deepa Deswal, Matti Karp, and Ramesh Chander Kuhad. "Bioprocessing of enhanced cellulase production from a mutant of Trichoderma asperellum RCK2011 and its application in hydrolysis of cellulose." *Fuel* 124 (2014): 183-189. https://doi.org/10.1016/j.fuel.2014.01.107

[29] Li, Xue, Wenming Li, Rufeng Zhang, Tao Jiang, Houhe Chen, and Guoqing Li. "Collaborative scheduling and flexibility assessment of integrated electricity and district heating systems utilizing thermal inertia of district heating network and aggregated buildings." *Applied Energy* 258 (2020): 114021. https://doi.org/10.1016/j.apenergy.2019.114021

[30] Broumand, Mohsen, Muhammad Shahzeb Khan, Sean Yun, Zekai Hong, and Murray J. Thomson. "Feasibility of running a micro gas turbine on wood-derived fast pyrolysis bio-oils: Effect of the fuel spray formation and preparation." *Renewable Energy* 178 (2021): 775-784. https://doi.org/10.1016/j.renene.2021.06.105

[31] Anufriev, I. S., S. V. Alekseenko, O. V. Sharypov, and E. P. Kopyev. "Diesel fuel combustion in a direct-flow evaporative burner with superheated steam supply." *Fuel* 254 (2019): 115723. https://doi.org/10.1016/j.fuel.2019.115723

[32] Allouis, C. H. R. İ. S. T. O. P. H. E., A. Amoresano, R. Capasso, G. Langella, V. Niola, and G. Quaremba. "The impact of biofuel properties on emissions and performances of a micro gas turbine using combustion vibrations detection." *Fuel Processing Technology* 179 (2018): 10-16. https://doi.org/10.1016/j.fuproc.2018.06.003

[33] Enagi, Ibrahim Idris, Khaled Ali Al-attab, and Zainal Alimuddin Zainal Alauddin. "Combustion stability analysis of liquid biofuels using acoustic signals." *Journal of Advanced Research in Fluid Mechanics and Thermal Sciences* 76, no. 1 (2020): 145-155. https://doi.org/10.37934/arfmts.76.1.145155

[34] Tan, Nurfarah Diana Mohd Ridzuan, Fudhail Abdul Munir, Musthafah Mohd Tahir, Herman Saputro, and Masato Mikami. "Preliminary investigation of using DBD plasma for application in micro combustors." *Journal of Advanced Research in Fluid Mechanics and Thermal Sciences* 82, no. 1 (2021): 105-112. https://doi.org/10.37934/arfmts.82.1.105112

[35] Taib, Norhidayah Mat, Mohd Radzi Abu Mansor, and Wan Mohd Faizal Wan Mahmood. "Simulation of Hydrogen Fuel Combustion in Neon-oxygen Circulated Compression Ignition Engine." *Journal of Advanced Research in Numerical Heat Transfer* 3, no. 1 (2020): 25-36.

[36] Sewucipto, Sanjaya, and Triyogi Yuwono. "The Influence of Upstream Installation of D-53 Type Cylinder on the Performance of Savonius Turbine." *Journal of Advanced Research in Experimental Fluid Mechanics and Heat Transfer* 3, no. 1 (2021): 36-47.

[37] Saha, Avijit, Temistocle Grenga, Abhishek Y. Deshmukh, Jörn Hinrichs, Mathis Bode, and Heinz Pitsch. "Numerical modeling of single droplet flash boiling behavior of e-fuels considering internal and external vaporization." *Fuel* 308 (2022): 121934. https://doi.org/10.1016/j.fuel.2021.121934

[38] Zhang, Chunhua, Ke Yang, Gang Li, Jiayi Dai, and Timothy H. Lee. "Spray evaporation characteristics of isopropanol-butanol-ethanol (IBE)/diesel blends in a constant volume chamber." *Fuel* 330 (2022): 125659. https://doi.org/10.1016/j.fuel.2022.125659

[39] Fredrich, Daniel, Erik Weiand, and Andrea Giusti. "Electrostatic fields for the control of evaporating charged fuel sprays." *International Journal of Multiphase Flow* 160 (2023): 104312. https://doi.org/10.1016/j.ijmultiphaseflow.2022.104312

[40] Ilhan, Beybin, Melike Kurt, and Hakan Ertürk. "Experimental investigation of heat transfer enhancement and viscosity change of hBN nanofluids." *Experimental Thermal and Fluid Science* 77 (2016): 272-283. https://doi.org/10.1016/j.expthermflusci.2016.04.024

[41] Gheidan, Abdelgader Agilah Saleh, Mazlan Abdul Wahid, and Mohd Fairus Mohd Yasin. "Investigations on Emission Characteristics of Methane in Small Scale a Swirl Flameless Combustor: Using Preheating Air Diluted CO2 and N2 Gas at Various Temperatures." *Journal of Advanced Research in Fluid Mechanics and Thermal Sciences* 100, no. 2 (2022): 113-137. https://doi.org/10.37934/arfmts.100.2.113137

[42] Zulkurnai, Fatin Farhanah, Norhidayah Mat Taib, Wan Mohd Faizal Wan Mahmood, and Mohd Radzi Abu Mansor. "Combustion characteristics of diesel and ethanol fuel in reactivity controlled compression ignition engine." *Journal of Advanced Research in Numerical Heat Transfer* 2, no. 1 (2020): 1-13.

[43] Abdulwahab, Mohammed Raad, Khaled Ali Mohammad Al-attab, and Mohamad Yusof Idroas. "Design and Characteristics of a New Pre-Evaporation Chamber Geometry for Low-Grade Palm Oil Fuel Evaporation for Micro Gas Turbine Application." *Journal of Advanced Research in Fluid Mechanics and Thermal Sciences* 94, no. 2 (2022): 184-199. https://doi.org/10.37934/arfmts.94.2.184199

[44] Delgado, Nacarid, Fredy Ysambertt, Gerson Chávez, Bélgica Bravo, Danny E. García, and Jorge Santos. "Valorization of kraft lignin of different molecular weights as surfactant agent for the oil industry." *Waste and Biomass Valorization* 10 (2019): 3383-3395. https://doi.org/10.1007/s12649-018-0352-4

[45] Awalludin, Mohd Fahmi, Othman Sulaiman, Rokiah Hashim, and Wan Noor Aidawati Wan Nadhari. "An overview of the oil palm industry in Malaysia and its waste utilization through thermochemical conversion, specifically via liquefaction." *Renewable and Sustainable Energy Reviews* 50 (2015): 1469-1484. https://doi.org/10.1016/j.rser.2015.05.085

[46] CHEMPRO-2021. Chempro-Edible-Oil Refining. http://chempro.in/palmoilproperties.htm

[47] Helena, L., A. A. Azira, and Mohamad Rusop. "Effect of Nickel Catalyst on Carbon Nanotubes by using Palm Oil as a Starting Material." *Advanced Materials Research* 667 (2013): 354-358. https://doi.org/10.4028/www.scientific.net/AMR.667.354